Geology and structure of the Serre Massif upper crust: a look in to the late-Variscan strike–slip kinematics of the Southern European Variscan chain

G. Ortolano, M. Pagano, R. Visalli, G. Angì, A. D'Agostino, F. Muto, V. Tripodi, S. Critelli & R. Cirrincione

View supplementary material

Published online: 26 Apr 2022.

Submit your article to this journal

Article views: 1736

View related articles

View Crossmark data

Citing articles: 5 View citing articles

SCIENCE

Geology and structure of the Serre Massif upper crust: a look in to the late-Variscan strike–slip kinematics of the Southern European Variscan chain

G. Ortolano[a], M. Pagano[a], R. Visalli[a], G. Angì[a], A. D'Agostino[a], F. Muto[b], V. Tripodi[b], S. Critelli[b] and R. Cirrincione[a]

[a]Dipartimento di Scienze Biologiche, Geologiche ed Ambientali – Sezione di Scienze della Terra, Università degli Studi di Catania, Corso Italia, Italy; [b]Dipartimento di Biologia, Ecologia e Scienze della Terra – Sezione di Scienze della Terra, Università della Calabria, Arcavacata di Rende (CS), Italy

ABSTRACT
A new geological-structural map of the southern Serre Massif (SM), in the south-central part of the Calabrian-Peloritani-Orogen (CPO), is provided. CPO is a ribbon-like microplates puzzle, originally belonging to the southern European Variscan Belt and, later involved into the Alpine geodynamics of the central Mediterranean Area. The SM represents one of the key European Variscan basement relicts, because of its exhumation mechanisms as well as for the absence of any Alpine metamorphic overprint. This map has the aim to better delineate the sequence of the Variscan blasto-deformational relationships consisting in a prograde multistage history, followed by an extensional/transpressional multistage retrograde evolution, which triggered the intrusion of the former plutonic products. The mylonitic fabric resulted finally replaced by the effects of the late- to post-kinematic plutonic intrusions coeval with a former late-Variscan exhumation stage, followed, during Mesozoic, by carbonate platform sedimentation, before to be completed exhumed during the Oligocene-Miocene Alpine stages.

1. Introduction

Structural, microstructural, and petrographic analysis of basement rocks, allows the reconstruction of the crosscutting relationships as well as of the rheological behaviours of each deformational stage, permitting, in turn, to define the correct sequence of the paragenetic equilibria useful to obtain reliable thermobarometric constraints (e.g. Corti et al., 2017, 2019; Fazio et al., 2015a; Gosso et al., 2010, 2015, 2019; Johnson & Vernon, 1995; Lardeaux & Spalla, 1991; Ortolano et al., 2015; Roda et al., 2021; Spalla, 1993; Spalla et al., 2005; Zucali et al., 2002, 2015, 2020). In other words, it represents the cornerstone for reconstruction of the ancient deep Earth crust kinematics.

In the western Mediterranean region, most of the basement rocks are nowadays exposed as the result of the combined effects of exhumation processes started during the latest stages of the Variscan orogeny (~300 Ma; e.g. Angì et al., 2010; Festa et al., 2013, 2020; Liotta et al., 2004, 2008; Martínez Catalán et al., 2009; Molli et al., 2020; Ortolano et al., 2020a; Tursi et al., 2020) (Figure 1(a)), completed during the Oligocene-Miocene Alpine evolutionary stages (e.g. Brandt & Schenk, 2020; Cirrincione et al., 2012a; Critelli, 2018; Fazio et al., 2018; Festa et al., 2020; Malusà

et al., 2015; Ortolano et al., 2005, 2020a, 2020b; Pezzino et al., 2008; Rosenbaum et al., 2002; Rossetti et al., 2001, 2004) (Figure 1(b)). These Variscan basement complexes were originally aligned along the suture zone formed as a consequence of the northward migration of Gondwana and peri-Gondwanan terranes (i.e. Avalonia, Armorica), started in lower Carboniferous (~360 Ma), which caused the closure of the Rheic Ocean, and the continental collision with Laurussia plate with the final amalgamation of Pangaea (~300 Ma) (Stampfli & Borel, 2002; Stampfli & Kozur, 2006; von Raumer et al., 2009).

The initial crustal thickening stage, averagely aged from 360 to 340 Ma (e.g. Fornelli et al., 2020), was followed by the activation of deep-seated strike-slip shear zones, within an overall contraction regime, linked to the mutual movement of Gondwana and Laurussia, operating from 344 to 300 Ma (Figure 1(a)).

These shear zones experienced the development of coeval transpressional and transtensional tectonics (Corsini & Rolland, 2009; Faure et al., 2010; Padovano et al., 2012; Pereira et al., 2010), driven by non-linear fault systems also known in literature as 'snake faults' (Elter et al., 2010) (Figure 1(a)). One of the most important of these shear zones was the Eastern Variscan Shear Zone (EVSZ), which
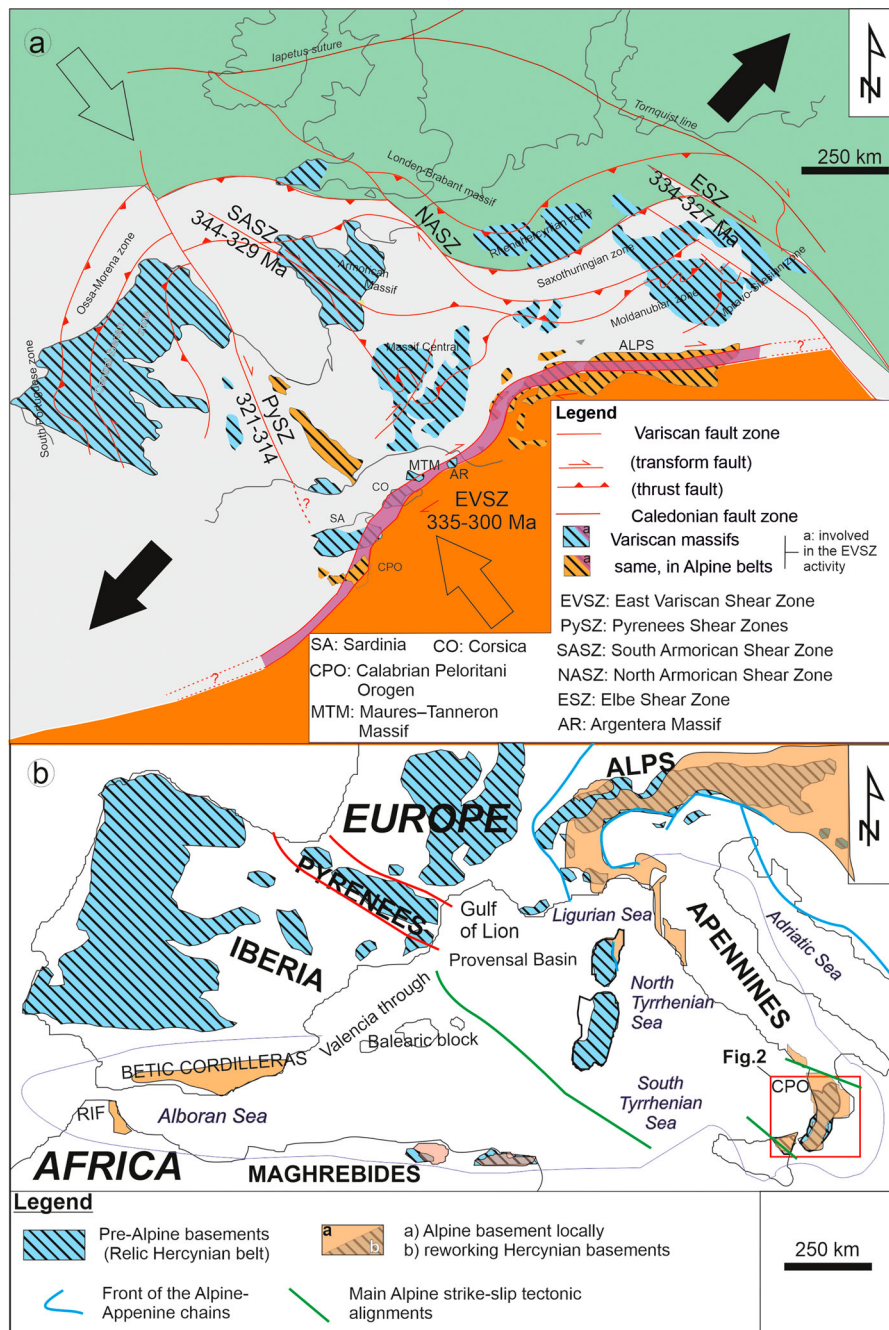
Figure 1. Past and present geodynamic scenario of the western Mediteranean realm (a) Frame of the western Mediterranean strike-slip kinematic pattern in the Late Carboniferous–Early Permian time interval. Green area Laurussia geodynamic domain; gray area: Gondwana derived microplates; orange area: Gondwana plate. EVSZ: East Variscan Shear Zone (Corsini & Rolland, 2009; Padovano et al., 2012); PySZ: Pyrenees Shear Zones; SASZ: South Armorican Shear Zone (Tartèse et al., 2012); NASZ: North Armorican Shear Zone; ESZ: Elbe Shear Zone (Hofmann et al., 2009); CPO: Calabria-Peloritani-Orogen (Cirrincione et al., 2012a); Sa: Sardinia; Co: Corsica; MTM: Maures–Tanneron Massif; Big white arrow (Palinspastic reconstruction of the main contractional regional stress axis); Big black arrow (Palinspastic reconstruction of the main extensional regional stress axis) (modified after Franke, 2000; Matte, 2001; Padovano et al., 2014; von Raumer et al., 2003). (b) Present-day distribution of the Alpine and Pre-Alpine Basement in western Europe with CPO location and main Alpine strike-slip tectonic alignment (after Cirrincione et al., 2015).

involved numerous Variscan massifs scattered in the western Mediterranean region (Carosi et al., 2020; Padovano et al., 2012; 2014). EVSZ activity led to the development of regional mylonitic foliation locally associated with syn- to late tectonic plutonic intrusions of Permian age (e.g. Angì et al., 2010; Cirrincione et al., 2015; De Vivo et al., 1991; Elter et al., 2010; Fazio et al., 2014; Fazio et al., 2020; Fiannacca et al., 2008, 2015, 2017, 2019, 2021; Liotta et al., 2008; Rottura et al., 1990, 1991).

The following Pangaea breakup, starting with the development of the Central Atlantic Magmatic Province (CAMP) (e.g. Cirrincione et al., 2013), signed the switch from a contraction to an extensional

regime, controlling the formation of Eurasia and African plates, as well (Faure et al., 2010; Matte, 2001; Melleton et al., 2010; Stampfli & Borel, 2002; Stampfli & Kozur, 2006; von Raumer et al., 2009).

The subsequent counter-clockwise rotation of the African plate triggered the former stages of the Alpine orogenesis, causing the further fragmentation of the original southern European Variscan chain. This stage was favored by the activation of new crustal-scale shear zones which controlled the Oligocene-Miocene microplates movement of the western Mediterranean realm (Figure 1(b) and Figure 2) (Brandt & Schenk, 2020; Cirrincione et al., 2015; Festa et al., 2016, 2020; Ortolano et al., 2020a).

In this geodynamic scenario, is born the Calabria-Peloritani-Orogen (CPO), mostly interpreted as a southward shifted fragment of the original European continent, drifted, in the present-day position, as a consequence of the slab roll-back of the subducting Ionian microplate (i.e. a relic of the neo-Thetyan oceanic crust) (Haccard et al., 1972; Malinverno & Ryan, 1986), controlling also the opening of the Tyrrhenian basin (Figure 1(b)).

The unitary geodynamic evolution of the CPO basements units is still discussed by various authors (e.g. Alvarez & Shimabukuro, 2009; Cirrincione et al., 2015; Critelli, 2018; Critelli et al., 2017), that distinguished at least two main sectors: (a) the northern sector, including the Catena Costiera and Sila Massif, where oceanic units are located between the overlying pre-Mesozoic continental crustal rocks and the underlying carbonate Apennine units (Appendix 1 – Geological framework); and (b) the southern sector, including the Serre and Aspromonte Massifs in the central-southern Calabria and the Peloritani Mountains in the north-eastern Sicily, where only continental crust-derived units occur (Appendix 1 – Geological framework).

Within the southern CPO it is possible further subdivide the Serre Massif from the Aspromonte and Peloritani Mountains, in view of the pervasive Oligocene Alpine metamorphic overprint recognized only in the central and eastern sector of the Aspromonte Massif (Cirrincione et al., 2008, 2015; Fazio et al., 2015b, 2018, 2020; Ortolano et al., 2005, 2015; Pezzino et al., 2008) and along the boundary between the two uppermost units of the Peloritani Mountains (Cirrincione et al., 2012a). The Serre Massif is indeed devoid of any Alpine metamorphic overprint and it is constituted by an almost complete continental crustal section, totally surfacing after an asymmetric tilting, due to the extensional (Festa et al., 2013) vs. transpressional exhumation (Fiannacca et al., 2021) of the original southern European Variscan basement (Cirrincione et al., 2008, 2012a, 2015; Fazio et al., 2018; Ortolano et al., 2015).

In particular, this new geological-structural map delineates the boundary among the intermediate (i.e. the late Variscan granitoids), to the upper portion (i.e. the SPC and the MPC) of the Serre Massif metamorphic crustal section, and its Mesozoic sedimentary sequence (Figure 2), with a special look into the exhumation mechanisms of this original southern European Variscan basement crust.

2. The geological-structural map of the Serre Massif upper crust

2.1. General outlines

The geological-structural map of the southern Serre Massif covers an area of ~290 km^2 in the CPO central-southern edge, and represents a revised merge of two original geological surveys (1:10000 scale).

Base map consists of contour lines (drawn every 50 m, labeled every 100 m), derived from the Digital Terrain Model (DTM) downloaded from the geodata website of the Calabrian Region (5 meters per pixel), also used to obtain the used hillshade effect (i.e. a virtual shaded relief) as well as the others geomorphological features (see supplementary material-SM1).

This new geological-structural map holds detailed information related to the tectono-metamorphic, -magmatic and -sedimentary evolution of the upper continental crust of the Serre Massif crustal section (Figure 2). The metamorphic and plutonic complexes here outcropping are mainly characterized by the superposition of an upper low-grade metamorphic complex (Stilo-Pazzano Complex – SPC) on a relatively high-grade metamorphic one (Mammola Paragneiss Complex – MPC), along a late-Variscan low-angle tectonic detachment (Figure 2) (Appendix 1; 2). Both the complexes share the same static metamorphic overprint related to the contact metamorphism due to the emplacement of the late-Variscan plutonic suite of the Serre Batholith (Angì et al., 2010; Bonardi et al., 1987; Cirrincione et al., 2012b; Festa et al., 2013; Fiannacca et al., 2015, 2017, 2019; Rottura et al., 1990), followed by the final intrusion of late to post-Variscan felsic to mafic dykes (Romano et al., 2011).

The map runs along the preserved primary boundary between the Serre Batholith and the metamorphic units, along which, a variably thick contact aureole occurs (Appendix 2).

To the south, the map intercepts the geological boundary between the Serre and the Aspromonte Massifs, where an already active deep-seated strike-slip fault system occurs. According to Ortolano et al. (2013, 2020a), Cirrincione et al. (2015) and Tripodi et al. (2018), this strike-slip system was recently interpreted as the natural continuation of the meso- to neo-
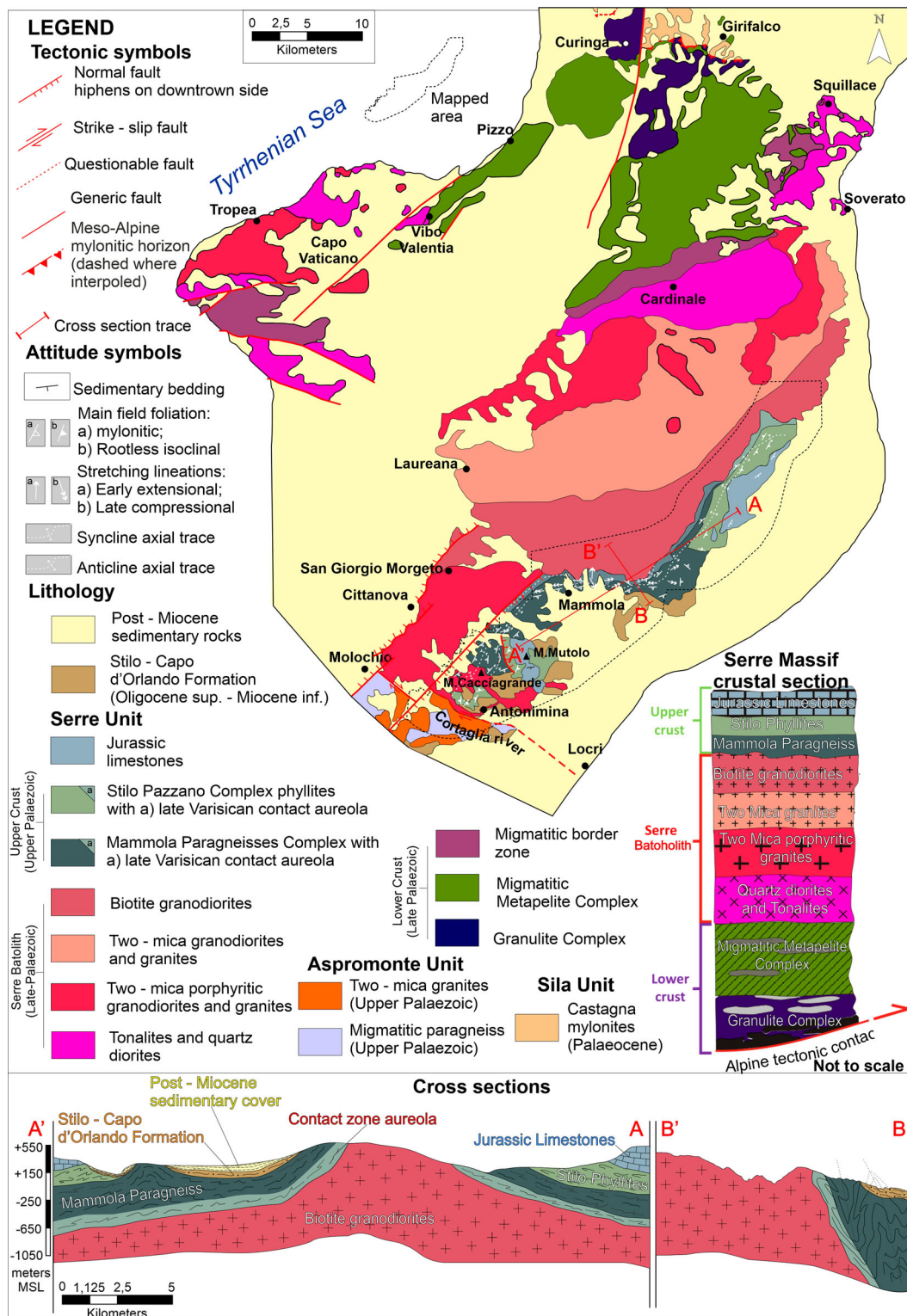
Figure 2. Geological sketch map of the Serre Massif with location of the mapped area.

Alpine strike-slip mylonitic Palmi Shear Zone (Appendix 1 – Geological framework).

2.2. Mammola paragneiss complex (MPC)

The MPC rocks crop out in the central part of the map with continuity from Mammola Village to Mt S. Andrea, and subordinately in the westernmost part. It is mainly composed of a paragneiss-micaschist sequence with local leucocratic orthogneiss and subordinate meter intercalations of amphibolite.

Field and microscopic investigations (see SM2) permitted the identification of two different metamorphic cycles: (a) an elder eo-Variscan polyphase syn-orogenic metamorphism ($D_1 \rightarrow M_1$ and $D_2 \rightarrow M_2$ phases) ended with a retrograde mylonitic evolution ($D_3 \rightarrow M_3$) followed by (b) a late- to post-tectonic

metamorphic overprint (M_4), caused by the intrusion of the late-Variscan granitoids.

The structural features are mainly linked to the retrograde shearing evolution of the first cycle ($D_3 \rightarrow M_3$), often characterized by transpressional-type structural features along the widely preserved pervasive subvertical foliations (Figure 3(a)). Kinematic indicators, lying on the XZ plane of the finite strain ellipsoid, are consistent with a dextral shear sense and an ENE tectonic transport in the present-day geographic coordinates (Figure 3(a–d)). Two different types of isoclinal fold sections lying on YZ plane of the finite strain ellipsoid are observed: (a) the first one is clearly in continuity with the mylonitic foliation with axes parallel to the stretching lineation, here interpreted as a syn-shearing oblique folding formation (Figure 3(e)) rather than a post-mylonitic isoclinal folding (Festa et al., 2018); (b) the second one, preserves an axial plane foliation S_1 in low strain domains lined up along the mylonitic foliation (Figure 3(f)). In the michaschist levels a centimeter wavelength microfolding forms a less developed S_2 foliation (Figure 3(g)).

Attitudes orientation pattern of the field foliation (S_3) maintains a similar distribution from the eastern-up to the western-sector of the central mapped area, showing a well-developed single girdle distribution of poles to planes, consistent with a folding system characterized by a sub-horizontal or less inclined axis, oriented from NE-SW to ENE-WSW (Figure 4 (a,b)) (Appendix 2). Obtained π axis is very well consistent with the b_4 measured axes (Figure 4(a,b)), which can be ascribed to a late-Variscan deformational stage D_4, due to the syn-compressional emplacement mechanism of the pluton, as testified also by the parallel orientation between the primary contact with granodiorite body and the average axis of the folding system (Figure 2) (Appendices 1, 2). Stretching-lineation L_3 shows a main ENE-WSW trend with a subordinate NE-SW one. The first one is parallel with the oblique-fold axes b_3 highlighting the syncinematism of both structures (Figure 3(e); Figure 4(a)), differently, the less preserved NE-SW L_3 trend can be interpreted as linked to an early-D_3 extensional deformative stage, alternatively plunging to NE or SW as response to the D_4 dispersion (Figure 2; Figure 4(a)).

2.3. Stilo-Pazzano complex (SPC)

The SPC includes lower greenschist facies metapelites interbedded with minor metalimestone and metabasite. It extends continuously along the north-eastern portion of the map, from Stilo, Pazzano and Bivongi to Popelli villages. Minor outcrops are in Caturello riverbed and near Martone village. Another important bodies of the SPC phyllites extensively crop outs at the base of the Mesozoic Monte Mutolo sedimentary sequence (Figure 5), as well as located between the two tributaries of the Antonimina River (i.e. The

Portigliola and Cortaglia rivers), where spotted phyllites crop outs directly in contact with the migmatitic paragneisses of the Aspromonte Unit. Similarly to the MPC, two metamorphic cycles have been recognized after field and microscopical investigations (see SM2): (a) an elder Variscan polyphasic regional metamorphism ($D_1 \rightarrow M_1$ and $D_2 \rightarrow M_2$ phases) followed by a less evident retrograde mylonitic stage ($D_3 \rightarrow M_3$ phase) and (b) a thermal overprint due to the intrusion of late-Variscan plutonic suite (M_4). The first deformational phase (D_1) determined an isoclinal folding (b_1 fold axes, spanning from a main NW-SE orientation to a subordinate E-W direction) (Figure 4(b)) of the S_0 surface, associated with the development of an axial plane foliation (S_1) (Figure 6(a)). The subsequent deformational stage (D_2) produced the crenulation of the S_1 with consequent micro-folding formation from centimetric- up to submillimetre-wavelength (Figure 6(b)). The D_2 stage is linked with the development of a new incipient to pervasive surface (S_2) and an axial culmination lineation (L_2) with very variable orientation spanning from the main NE-SW to NNE-SSW and a minor cluster oriented to SE (Figure 4(b)). The D_3 deformational stage experienced in MPC lithotypes is not well observable in the SPC rocks, even though, widespread unrooted lenses of isoclinal folds (Figure 6(c)) can be interpreted as linked with the same early-D_3 mylonitic phase already observed in the MPC. Moreover, the local preservation of sub-vertical foliation (Figure 6 (d)), can be linked to the late-D_3 transpressional phase well recognized in the MPC (Figure 6(d′)). The late-to post-kinematic intrusion of the plutonic body emplacement extensively produced spotted phyllites. This last metamorphic phase produced: (a) in peripheral contact aureole zone, 0.5–2 mm sized ellipsoidal cordierite spots, overgrowing locally on pre-existent fabrics; (b) approaching the contact, an abrupt texture variation with the transition to foliation-lacking hornfels, where cordierite gradually leaves the place to biotite and andalusite porphyroblasts (Figure 6 (e)) (Appendix 2).

The following D_4 deformational stage is correlated, also in this case, to the syn- to late-kinematic intrusion of the main granodiorite body, as testified by the same main rotation axis b_4 observed in the MPC, always sub-parallel with the primary contact with the granodiorite batholith. This suggests that the syn-compressional emplacement of the main plutonic body, caused the folding of the main foliation that, in the case of the SPC phyllites, correspond to a $S_1 \equiv S_3$ parallel foliation. Aplite-pegmatite dyke intrusions closed the second stage of the static cycle.

During the Mesozoic period, thin sea carbonate sediments were deposited on the SPC phyllites, interrupted by more or less wide gaps probably due to repeated emersion testified by paleosols or moderate

Figure 3. Field examples of lithotypes and structures from Mammola Paragneiss Complex. (a) Example of subvertical mylonitic foliation reporting finite strain ellipsoid sections with indication of the dextral shear sense (White circle on the upper left side indicates an inward movement relative to the observer. White circle on the upper right side indicates an outward movement relative to the observer). (b) Example of late-S_3 mylonitic foliation. (c) Sin-kinematic asymmetric intrafoliar fold showing dextral shear sense consistent with an ENE tectonic transport. Cutting according to the XZ ellipsoid section. (d) Mylonitic amphibolite levels (Monte Bruverello area). (e) Longitudinal oblique folds sections. Cutting according to the YZ ellipsoid section (B_3 is the axis of the oblique folding generated during the strike-slip movement. S_3 is the mylonitic field-foliation). (f) Axial plane foliation preserved within a relic of isoclinal folding (S_1 is the relic axial plane foliation preserved as low-strain domain within the S_3 mylonitic field-foliation. B_1 is the axis of the isoclinal folding event produced during the first recognized deformational phase D_1). (g) Subperpendicular foliation produced by a centimeter wavelength crenulation in micaschist levels (B_2 stay for wavelength centimeter axis produced during the D_2 event. See text for more explanation). (h) Post-tectonic paraconcordant dyke and late-tectonic dyke characterized by supra-solidus deformative structures (h''). (i) Discordant post-tectonic aplitic dyke.
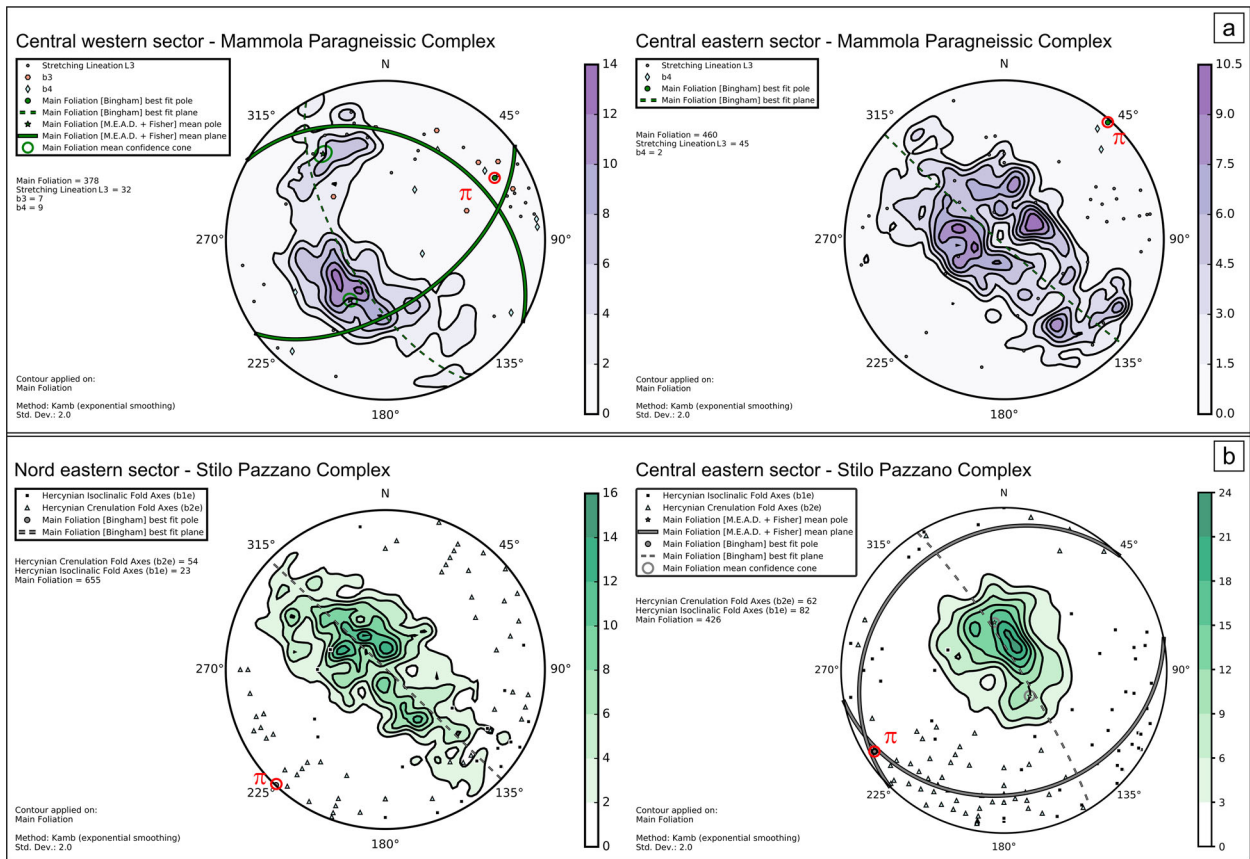
Figure 4. Structural data orientation patterns collected along the mapped area. Contouring and statistical analyses are computed on main foliation data by means of the tool ArcStereoNet (Ortolano et al., 2021). The π axes are statistically computed as the poles to Bingham best-fit planes. (a) MPC structural data collected on central western and central eastern sector, respectively. (b) SPC structural data collected on north-eastern and central-eastern sector, respectively.

thicknesses of 'Verrucano' type clastic deposits (Bonardi et al., 1984). This initial sedimentation was replaced by dolomite covered in turn by whitish and pearl-gray calcarenites and calcirudites, sometimes with a pinkish micritic matrix, breccias and reef limestones with ellipsactinias, corals and gastropods, and light gray calcarenites and calcirudites with Clypeina jurassica.

2.4. Aspromonte unit

The Aspromonte Unit (AU) lithotypes crop out only in the southwestern part of the map along the right bank of the Cortaglia river, along which an already active deep-seated strike-slip fault system, occurs (Apollaro et al., 2019) (Appendix 1). The lithotypes consist of migmatitic paragneisses (Figure 7(a,b)) intruded by

Figure 5. Panoramic landscape of the preserved original tectono-stratigraphic setting between SPC phyllites and Monte Mutolo limestones near Canolo town. MPC lithotypes are in contact along a tectonic detachment.

Figure 6. Field examples of lithotypes and structures belonging to the Stilo-Pazzano Complex. (a) Isoclinal folding of the original S_0 surface highlighted by the development of an axial plane foliation. (b–b') Centimeter- to submillimetre-wavelength crenulation on S_1 surface. (c) Unrooted lenses of isoclinal folds indicating an extensional shearing. (d–d') Sub-vertical foliation facilitating granite intrusion. (e) Centimetric static andalusite porphyroblast occurring near the plutonic contact. (f–f') Asymmetric folding with axis parallel to the preserved primary contact with main batholite intrusion.

Late-Variscan small-sized plutonites (Figure 7(c,d)), represented by syn- to post-tectonic magmatic bodies compositionally varying from monzogranites to fine-grained leucogranodiorites. These lasts are interpreted as different from the adjacent southern termination of the Serre Massif main plutonic body, principally, in view of the different host rocks, namely migmatitic paragneiss to the south of the Cortaglia alignment and phyllites just crossing the strike-slip system to the north) (Figure 6(d)).

The Cortaglia River tectonic alignment has an ENE–WSW orientation, and is evidenced by the
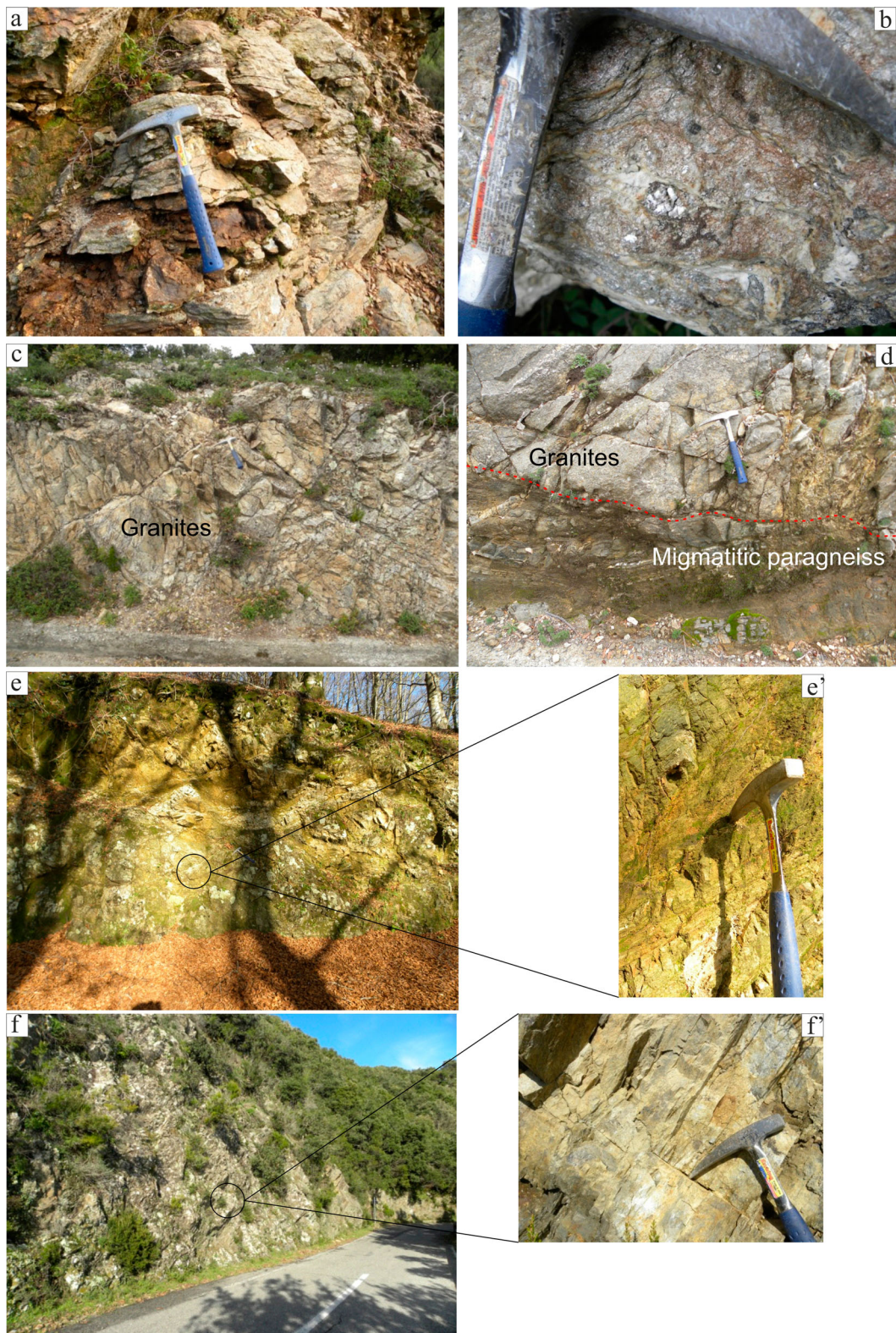
Figure 7. Field examples of lithotypes and structures belonging to the Aspromonte Unit. (a–b) Migmatitic paragneisses. (c–d) Late-Variscan small-sized granites intruding migmatitic paragneisses. (e–e') Unconsolidated ultracataclasites from granitoid parent rock near the Cortaglia tectonic alignment. (f–f') Mylonitic leucocratic orthogneisses characterized by the absence of recovery processes.

presence of strongly tectonized areas, characterized by unconsolidated ultracataclasites from granitoid parent rock (Figure 7(e,e')).

The differences between the rocks to the north and to the south of this tectonic alignment are highlighted by the occurrence, to the south, of mylonitic leuco-cratic orthogneisses characterized by a total absence of recovery processes (Figure 7(f,f')), very different from the mylonitic rocks of the MPC rocks, strongly recovered by the temperature increase due to the

late-Variscan plutonic body emplacement. This last evidence highlights as the development of the mylonitic fabric in the AU rock types is due to the late-Alpine overprint mainly preserved in the central-eastern part of the Aspromonte Massif (Bonardi et al., 1984; Cirrincione et al., 2008, 2015, 2017; Fazio et al., 2015b; 2018; Heymes et al., 2010; Ortolano et al., 2005; 2015; Pezzino et al., 1990; 2008; Platt & Compagnoni, 1990).

2.5. Post-Mesozoic *sedimentary succession*

2.5.1. Stilo-Capo d'Orlando formation
During the Apennine phase of the Alpine orogenesis, the Mesozoic sedimentary succession of the SPC was partly covered by the late Oligocene – early Miocene syn-orogenic deposition of the Stilo-Capo d'Orlando Formation. This formation consists of conglomerates produced by the action of flow of debris or masses (debris flow or mass flow) along submarine paleocanyons, of clays with silty intercalations, frequently engraved by channeled conglomerates, corresponding to slope deposits and from thick turbidite arenaceous layers (Bonardi et al., 2003). This rests directly on the crystalline basement and on the Mesozoic carbonate sedimentary succession, cropping out extensively along the eastern margin of the map.

2.5.2. Antisicilide Unit
The Antisicilide Unit lies, in tectonic contact, on the Stilo Capo d'Orlando formation (Gioiosa Ionica and Antonimina areas) and, locally, on the crystalline basement. The provenance and type of emplacement of the Antisicilide Unit are widely debated by numerous authors, results interposed between the Capo d'Orlando flysch and the Middle - Upper Miocene terrigenous succession. The Unit is dated Upper Cretaceous – Lower Miocene and is made up of variable lithologies grouped into: greenish-reddish pelites with a scaly texture, often in a chaotic position, intensely affected by shear phenomena.

2.5.3. San Pier Niceto Formation
It is a succession of Serravallian-Tortonian age, composed of different lithofacies characterized by frequent lateral-vertical variations. It is mainly constituted by a siliciclastic lithofacies consisting of homogeneous banks of coarse fossiliferous sands with Clypeaster sp. The sandstones locally contain conglomerates and have sedimentary structures of the turbidite type.

2.5.4. Basal limestones
The unit is made up of white-yellow vacuolar limestones and strata of stratified marly limestone, of metric thickness, with pelitic intercalations of centimeter thickness (Critelli et al., 2016). Sometimes there are intercalations of gypsumarenites and

gypsumsylthites with centimetric lamination. The limestones, of Messinian age, are organized in massive banks, slightly slow, of plurimetric thickness intercalations of clayey marl, sometimes laminated of centimeter.

2.5.5. Mount Canolo Formation
The Messinian age Monte Canolo Formation is composed, starting from the base, by sandy levels, subordinately gravelly, from moderately thickened to very thickened, of brown color; the layers have medium thickness, sometimes with lenticular geometries, generally supporting a sandy matrix, and conglomerates. They are polygenic and heterometric, from sub-angular to angular, subordinately sub-rounded, slightly to moderately cemented; the rounded clasts are made up of granite and gneiss, differently the more angular clasts derive from micaschists and phyllites (Critelli et al., 2016a, 2016b).

2.5.6. Calcarenites and Trubi
At the base of the formation there are generally calcareous-marly rhythms; this rhythmicity is referable to the Milankovitch cycles which give to the formation, a characteristic stratification with alternating gray and whitish levels of marls and very rich in calcareous plankton marly limestones (Zanclean-Piacenzian). This formation is well exposed to the south of the Fiumara Torbido. The position of this formation is generally paraconcordant on the Trubi Formation; however, the contact between the two stratigraphic units is locally erosive (Critelli et al., 2016a).

3. Discussion

This work synthetized two field surveys made during the PhD thesis of Angì (2008) and the field activities within the Geological and Geothematic Italian Cartohography Project (CARG) with the realization of the Sheet N°590 (Polino et al., 2015).

Results confirm that the Serre Massif differs considerably from the adjacent Aspromonte-Peloritani orogenic system, in view of the different tectonic structure (Appendix 1 – Geological framework) and the absence of any Alpine metamorphic overprint. This is testified, for instance, by the different recognized mylonitic fabric where: (a) Aspromonte Unit mylonites, linked to the compressive late-Alpine mylonitic event built-up the Aspromonte Massif nappe-like edifice, are characterized by scanty recrystallized ribbon-like quartz levels (Figures SM3b′; b″) (Pezzino et al., 2008); (b) Serre Massif mylonites, linked with the late-Variscan strike-slip deformation subsequently interested by late- to post-kinematic granitoid emplacement, are instead characterized by strongly recovered ribbon-

like quartz levels (Figure SM3a′; a″) (Cirrincione et al., 2015).

This late-Variscan retrograde mylonitic phase, better recognized in the MPC rather than in the SPC was here subdivided into an early extensional retrograde stage, mostly visible at the thin section scale (SM2), followed by a transpressional stage, which probably triggered the initial plutonic body intrusion.

This hypothesis is also supported by recent studies on the Serre Massif batholite construction characterized by an overaccretion mechanism (Fiannacca et al., 2017), rather than a dominant extensional uplift controlled by a core complexing model exhumation (Festa et al., 2013), as testified by the clear granitoid deformation microstructures from submagmatic to low-temperature sub-solidus conditions, characterized by an internal granitoid fabric consistent with a shortening axis roughly oriented NW–SE, constrained by Anisotropy of magnetic susceptibility (AMS) study (Fiannacca et al., 2021). The NW-SE shortening axis observed in the granitoid bodies can be strictly correlated with the attitudes orientation pattern of the mylonitic field foliation (S_3) which maintains a distribution of poles to planes consistent with a folding system characterized by a sub-horizontal or less inclined axis, oriented from NE-SW to ENE-WSW and by stretching-lineation L_3 characterized by a main

ENE-WSW trend (Figure 4(a,b)) (Appendix 2); structures constantly consistent with the activity of a dextral type strike-slip tectonics, which can be ascribed to the late-D_3 transpressional stage and in line with the palinspastic reconstruction of the EVSZ activity (Figure 1(a)).

In this new tectonic framework the Serre Massif can be considered as belonged to the same geodynamic realm scattered throughout the Alps, the Corsica-Sardinia-Maures-Tanneron Massif, and the Northern Apennines, until late-Carboniferous time (Figure 1 (a)), where, during the interval from 330 to 300 Ma, the activity of the EVSZ affected all these massifs, locally triggering the emplacement of the late-Variscan granitoids, playing a key role in the evolution of the subsequent Alpine-Apennine cycle, acting as a pre-existing tectonic barrier (Carosi et al., 2020).

More in particular, the upper crustal levels of the Serre Massif geological evolution can be subdivided into an orogenic metamorphic cycle where the first deformational stage (D_1) is associated with the development of a penetrative and pervasive surface (S_1), more evident in the SPC rather than in the MPC rocks where it is preserved as relict isoclinal fold hinges within mylonitic foliation (Figure 3(f); Figure 6(a); Figure 8). D_1 is followed by a D_2 crenulation stage, better observable in the SPC rocks (Figure 6(b); Figure 8). These two prograde stages,
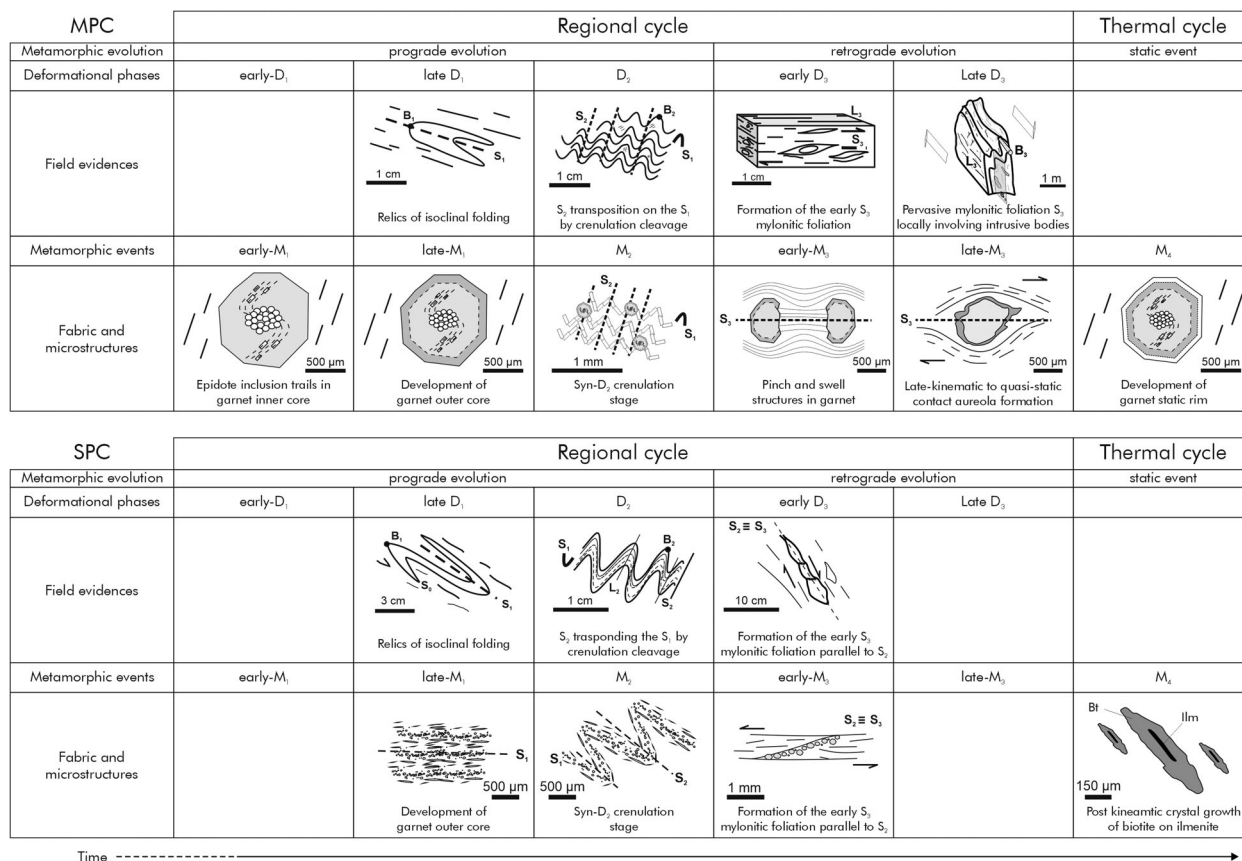

Figure 8. Synoptic reconstruction of the field- and petrographic-related evidence of the tectono-metamorphic evolution of the Mammola Paragneiss- and Stilo-Pazzano - metamorphic complexes.

consistent with the eo-Variscan crustal thickening phase, were followed by an early-retrograde extensional mylonitic stage (early-D$_3$), linked with the collapse of the orogen and a consequent crustal thinning stage, which brought also to the detachment of the more surficial levels of the original crustal section sequence (i.e. SPC) from the more high-grade MPC. This former extensional tectonic detachment was followed, in turn, by the mostly preserved transpressional stage, with the formation of an extensively pervasive mylonitic foliation (Figure 3(a–e); Figure 8). This last event triggers pluton intrusion which, in its former emplacement stage, was involved in the same stress field of the late-D$_3$ mylonitic stage, as suggested by the occurrence of late-tectonic dykes characterized by clear evidence of supra-solidus deformative structures (Figure 3(h,h′)) and confirmed by the same regional shortening axis consistent with the dextral shear-sense tectonics both in the basement rocks and in the granitoids. Finally, the late-Variscan plutonic emplacement continued with post-tectonic intrusion of paraconcordant (Figure 3(h)) to discordant dykes (Figure 3(i)), characterized by sharp contacts and devoid of any evidence of supra- or sub-solidus deformations.

4. Conclusion

The new geological map of the southern Serre Massif is a useful contribution to the geodynamic reconstruction of the late-Paleozoic scenario of the southern European Variscan belt: it permits to delineate the sequence of the Variscan metamorphic evolution, where, after a prograde multistage metamorphism, follow a pervasive retrograde evolution, controlled by an initial extensional mylonitic stage, linked with the initial collapsing of the orogen, replaced by a transpressional mylonitic stage, which triggered the intrusion of the former plutonic products under the same stress field of the mylonitic event. Mylonites were finally sutured by the late- to post-kinematic granitoid intrusion, producing *quasi*-static overprints with the recovery of the mylonitic fabric, before being exhumed, for the first time, at the end of the Palaezoic with the 'Verrucano' sedimentation, before to be covered by the Mesozoic carbonate platform sedimentation, and definitively exhumed at the end of the Oligocene with the unrooting from its original Variscan basement crust contemporaneously to the deposition of the syn-orogenic Stilo Capo d'Orlando formation and the backthrusting of the Antisicilide unit.

Software

The geological-structural map of the Serre Massif upper crust was mainly designed by means of the ArcGIS® software. In fact, thanks to its functionalities of data managing and storing, ArcGIS® allowed the map digitization and the database structuring to be properly accomplished.

Taking advantage of specific ArcGIS® toolboxes, such as 'Hillshade' and 'Contour', the extrapolation of useful topographical features from DTM was performed. Moreover, thanks to a new ArcGIS-based Python-toolbox (i.e. ArcStereoNet – Ortolano et al., 2021), the collected structural data have been studied with statistical analysis techniques and then plotted within lower-hemisphere equal-area stereonets. The statistical algorithms applied to data include density contour functions, clustering, and mean vectors extraction, together with the classic cluster and girdle analysis techniques (e.g. M.E.A.D. + Fisher and Bingham algorithms – see Ortolano et al., 2021 for details).

Since it operates within the ArcGIS® environment, ArcStereoNet merges its data analysis and plotting functionalities with the classic GIS features, including various data selection tools. In this view, the Graph To Hyperlink tool (included within the ArcStereoNet toolbox), which allows connecting via hyperlink the results of statistical analysis with the geographic location of the selected structural data, was used to extract and display the mean field foliations and the stretching lineations along the entire map (Appendix 2). Firstly, the structural data were manually grouped based on their geographic location. Consequently, the mean azimuth/dip values were extracted for each group and displayed at the corresponding centroid coordinates of the group. Finally, only the statistically consistent main foliation average values were maintained (i.e. those extracted from a number of data greater than 20 units).

The final editing and assemblage of map, geological sections, stereoplots, legends, and any other graphical element were accomplished by means of the GIMP software.

Data

The supplementary materials include a detailed description of the petrographical and geomorphological features of the over 120 samples from the mapped area and three explanatory figures.

Acknowledgements

References

Alvarez, W., & Shimabukuro, D. H. (2009). The geological relationships between Sardinia and Calabria during Alpine and Hercynian times. *Bollettino Della Società Geologica Italiana*, *128*(2), 257–268. https://doi.org/10.3301/IJG.2009.128.2.257

Angì, G. (2008). *Evoluzione Tettono-Metamorfica del Basamento Cristallino delle Serre Meridionali (Calabria Meridionale)* [Doctoral dissertation, http://hdl.handle.net/10761/2684

Angì, G., Cirrincione, R., Fazio, E., Fiannacca, P., Ortolano, G., & Pezzino, A. (2010). Metamorphic evolution of preserved Hercynian crustal section in the Serre Massif (Calabria–Peloritani Orogen, Southern Italy). *Lithos*, *115*(1–4), 237–262. https://doi.org/10.1016/j.lithos.2009.12.008

Apollaro, C., Tripodi, V., Vespasiano, G., De Rosa, R., Dotsika, E., Fuoco, I., Critelli, S., & Muto, F. (2019). Chemical, isotopic and geotectonic relations of the warm and cold waters of the Galatro and Antonimina thermal areas, southern Calabria, Italy. *Marine and Petroleum Geology*, *109*, 469–483. https://doi.org/10.1016/j.marpetgeo.2019.06.020

Bonardi, G., Compagnoni, R., Del Moro, A., Messina, A., & Perrone, V. (1987). Riequilibrazioni tettonico meta-morfiche alpine dell'Unita dell'Aspromonte, Calabria Meridionale. *Rendiconti della Società Italiana di Mineralogia e Petrologia*, *42*, 301.

Bonardi, G., Compagnoni, R., Messina, A., & Perrone, V. (1984). Riequilibrazioni metamorfiche di probabile età alpina nell'Unita dell'Aspromonte–Arco Calabro Peloritano. *Rendiconti della Società Italiana di Mineralogia e Petrologia*, *39*, 613–628.

Bonardi, G., De Capoa, P., Di Staso, A., Estévez, A., Martín-Martín, M., Martín-Rojas, I., Perrone, V., & Tent-Manclús, J. E. (2003). Oligocene-to-Early Miocene depositional and structural evolution of the Calabria–Peloritani Arc southern terrane (Italy) and geodynamic correlations with the Spain Betics and Morocco Rif. *Geodin. Acta*, *16*(2–6), 149–169. https://doi.org/10.1016/j.geoact.2003.06.001

Brandt, S., & Schenk, V. (2020). Metamorphic response to Alpine thrusting of a crustal-scale basement nappe in southern Calabria (Italy). *Journal of Petrology*, *61*(11-12), 1–39, egaa063, https://doi.org/10.1093/petrology/egaa063

Carosi, R., Petroccia, A., Iaccarino, S., Simonetti, M., Langone, A., & Montomoli, C. (2020). Kinematics and timing constraints in a transpressive tectonic regime: The example of the posada-asinara shear zone (NE Sardinia, Italy). *Geosciences (Switzerland)*, *10*(8), 288, 1–29. https://doi.org/10.3390/geosciences10080288

Cirrincione, R., Fazio, E., Fiannacca, P., Ortolano, G., Pezzino, A., & Punturo, R. (2012b). Quartz annealing microstructures in sheared rocks from the Serre Massif (Calabria, Italy). *Rendiconti Online Società Geologica Italiana*, *21*, 126–128.

Cirrincione, R., Fazio, E., Fiannacca, P., Ortolano, G., Pezzino, A., & Punturo, R. (2015). The Calabria-Peloritani Orogen, a composite terrane in Central Mediterranean; its overall architecture and geodynamic significance for a pre-Alpine scenario around the Tethyan basin. *Periodico di Mineralogia*, *84*(3B), 701–749. https://doi.org/10.2451/2015PM0446

Cirrincione, R., Fazio, E., Ortolano, G., Pezzino, A., & Punturo, R. (2012a). Fault-related rocks: Deciphering the structural-metamorphic evolution of an accretionary wedge in a collisional belt, NE Sicily. *International Geology Review*, *54*(8), 940–956. https://doi.org/10.1080/00206814.2011.623022

Cirrincione, R., Fiannacca, P., Lustrino, M., Romano, V., & Tranchina, A. (2013). Late Triassic tholeiitic magmatism in Western Sicily: A possible extension of the Central Atlantic Magmatic Province (CAMP) in the Central Mediterranean area? *Lithos*, *188*, 60–71. https://doi.org/10.1016/j.lithos.2013.10.009

Cirrincione, R., Monaco, C., Ortolano, G., Ferranti, L., Barreca, G., Fazio, E., Pezzino, A., & Visalli, R. (2017). From ductile to brittle tectonic evolution of the Aspromonte Massif Field excursion of the Italian Group of Structural Geology - Catania. *Geological Field Trips*, *9*(2), 1–66. https://doi.org/10.3301/GFT.2017.03

Cirrincione, R., Ortolano, G., Pezzino, A., & Punturo, R. (2008). Poly-orogenic multi-stage metamorphic evolution inferred via P-T pseudosections: An example from Aspromonte Massif basement rocks (Southern Calabria, Italy). *Lithos*, *103*(3–4), 466–502, ISSN: 0024-4937, https://doi.org/10.1016/j.lithos.2007.11.001

Corsini, M., & Rolland, Y. (2009). Late evolution of the Southern European Variscan belt: Exhumation of the lower crust in a context of oblique convergence. *Comptes Rendus Geoscience*, *341*(2–3), 214–223. https://doi.org/10.1016/j.crte.2008.12.002

Corti, L., Alberelli, G., Zanoni, D., & Zucali, M. (2017). Analysis of fabric evolution and metamorphic reaction progress at lago della vecchia-valle d'irogna, sesia-lanzo zone, western alps. *Journal of Maps*, *13*(2), 521–533. https://doi.org/10.1080/17445647.2017.1331177

Corti, L., Zucali, M., Visalli, R., Mancini, M., & Sayab, M. (2019). Integrating X-Ray computed tomography with chemical imaging to quantify mineral re-crystallization from granulite to eclogite metamorphism in the Western Italian Alps (Sesia-Lanzo Zone). *Frontiers in Earth Science*, *7*, https://doi.org/10.3389/feart.2019.00327

Critelli, S. (2018). Provenance of Mesozoic to Cenozoic Circum-Mediterranean sandstones in relation to tectonic setting. *Earth-Science Reviews*, *185*, 624–648. https://doi.org/10.1016/j.earscirev.2018.07.001

Critelli, S., Muto, F., Perri, F., & Tripodi, V. (2017). Interpreting Provenance relations from Sandstone Detrital Modes, Southern Italy Foreland Region: Stratigraphic record of the miocene tectonic evolution. *Marine and Petroleum Geology*, *87*, 47–59. https://doi.org/10.1016/j.marpetgeo.2017.01.026
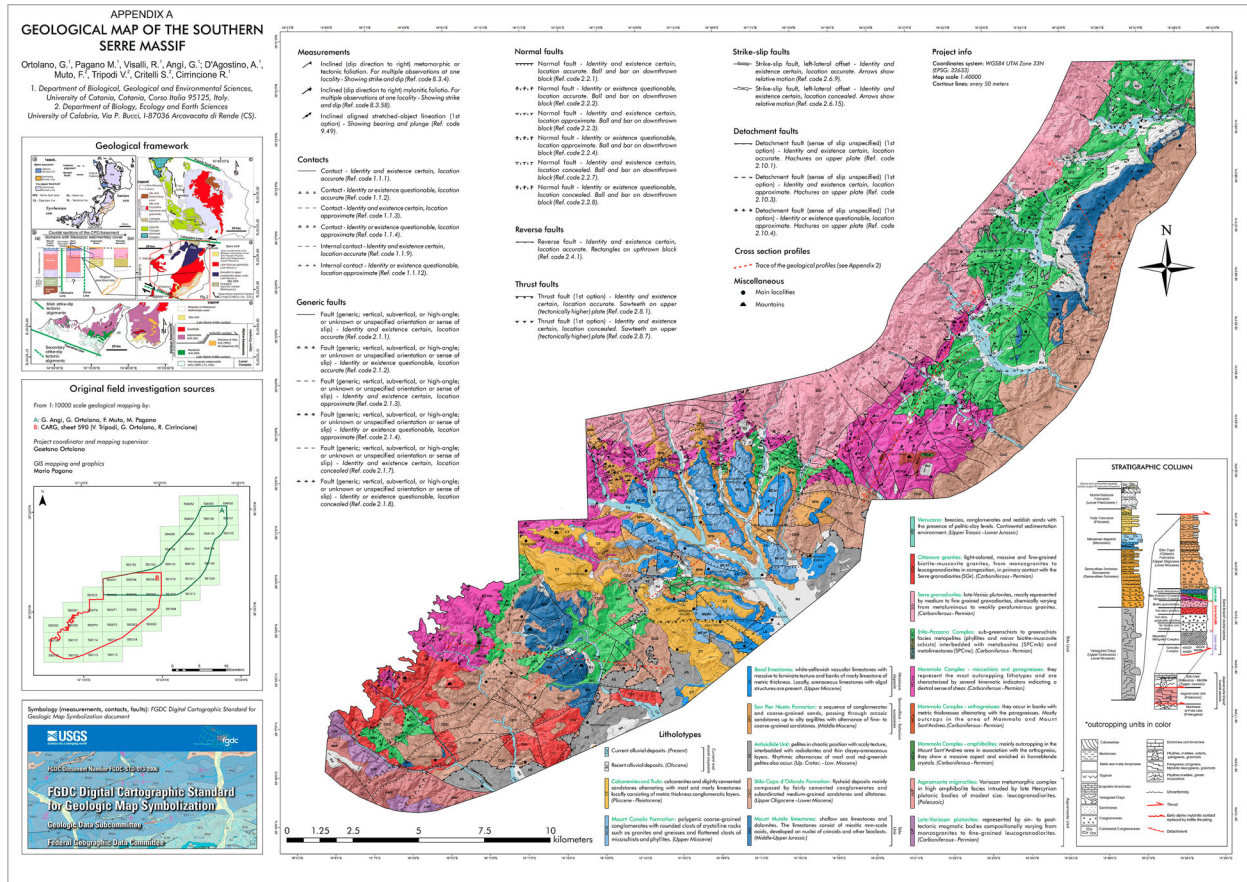
Critelli, S., Muto, F., & Tripodi, V. (2016a). Note illustrative della Carta Geologica D'Italia alla scala 1:50.000 foglio 603 Bovalino. ISPRA (Istituto Superiore per la Protezione e la Ricerca Ambientale), Servizio Geologico d'Italia, Progetto CARG.

Critelli, S., Muto, F., & Tripodi, V. (2016b). Note illustrative della Carta Geologica D'Italia alla scala 1:50.000 foglio 590 Taurianova. ISPRA (Istituto Superiore per la Protezione e la Ricerca Ambientale), Servizio Geologico d'Italia, Progetto CARG.

De Vivo, B., Ayuso, R. A., Belkin, H. E., Lima, A., Messina, A., & Viscardi, A. (1991). Rock chemistry and fluid inclusion studies as exploration tools for ore deposits in the Sila batholith, southern Italy. *Journal of Geochemical Exploration*, *40*(1–3), 291–310. https://doi. org/10.1016/0375-6742(91)90044-U

Elter, F. M., Padovano, M., & Kraus, R. K. (2010). The emplacement of Variscan HT metamorphic rocks linked to the interaction between Gondwana and Laurussia: Structural constraints in NE Sardinia (Italy). *Terra Nova*, *22*(5), 369–377. https://doi.org/10.1111/j.1365-3121.2010.00959.x

Faure, M., Cocherie, A., Mezeme, E. B., Charles, N., & Rossi, P. (2010). Middle Carboniferous crustal melting in the Variscan Belt: New insights from U–Th–Pb$_{tot}$. Monazite and U–Pb zircon ages of the Montagne Noire Axial Zone (southern French Massif Central). *Gondwana Research*, *18*(4), 653–673. https://doi.org/10.1016/j.gr.2010.02.005

Fazio, E., Cirrincione, R., & Pezzino, A. (2015b). Tectono-metamorphic map of the south-western flank of the Aspromonte Massif (southern Calabria –Italy). *Journal of Maps*, *11*(1), 85–100. https://doi.org/10.1080/17445647.2014.962634

Fazio, E., Fiannacca, P., Ortolano, G., Cirrincione, R., Punturo, R., & Mamtani, M. A. (2014). Integrating field, microstructural and AMS data to determine the time-relationship between granite emplacement and regional deformation: An example from Calabria (Italy). *Rock Deformation & Structures Conference: RDS-III-2014*, 83–84. https://doi.org/10.13140/2.1.3399.4568

Fazio, E., Fiannacca, P., Ortolano, G., Punturo, R., Zanoni, D., & Zucali, M. (2015a). Progresses in deciphering structures and compositions of basement rocks. *Periodico di Mineralogia*, *84*(3).

Fazio, E., Fiannacca, P., Russo, D., & Cirrincione, R. (2020). Submagmatic to solid-state deformation microstructures recorded in cooling granitoids during exhumation of late-Variscan crust in north-eastern Sicily. *Geosciences (Switzerland)*, *10*(8), 1–29. art. no. 311. https://doi.org/10.3390/geosciences10080311

Fazio, E., Ortolano, G., Visalli, R., Alsop, I., Cirrincione, R., & Pezzino, A. (2018). Strain localization and sheath fold development during progressive deformation in a ductile shear zone: A case study of macro-to micro-scale structures from the Aspromonte Massif, Calabria. *Italian Journal of Geosciences*, *137*(2), 208–218. https://doi.org/10.3301/IJG.2018.09

Festa, V., Caggianelli, A., Langone, A., & Prosser, G. (2013). Time–space relationships among structural and metamorphic aureoles related to granite emplacement: A case study from the Serre Massif (southern Italy). *Geological Magazine*, *150*(3), 441–454. https://doi.org/10.1017/S0016756812000714

Festa, V., Cicala, M., & Tursi, F. (2020). The Curinga–Girifalco line in the framework of the tectonic evolution of the remnant Alpine chain in Calabria (southern Italy). *International Journal of Earth Sciences*, *109*(7), 2583–2598. https://doi.org/10.1007/s00531-020-01918-5

Festa, V., Prosser, G., Caggianelli, A., Grande, A., Langone, A., & Mele, D. (2016). Vorticity analysis of the Palmi shear zone mylonites: New insights for the Alpine tectonic evolution of the Calabria–Peloritani terrane (southern Italy). *Geological Journal*, *51*(4), 670–681. https://doi.org/10.1002/gj.2673

Festa, V., Tursi, F., Caggianelli, A., & Spiess, R. (2018). The tectono-magmatic setting of the Hercynian upper continental crust exposed in Calabria (Italy) as revealed by the 1:10,000 structural-geological map of the Levadio stream area. *Italian Journal of Geosciences*, *137*(2), 165–174. https://doi.org/10.3301/IJG.2018.03

Fiannacca, P., Cirrincione, R., Bonanno, F., & Carciotto, M. M. (2015). Source-inherited compositional diversity in granite batholiths: The geochemical message of late Paleozoic intrusive magmatism in central Calabria (southern Italy). *Lithos*, *236*, 123–140. https://doi.org/10.1016/j.lithos.2015.09.003

Fiannacca, P., Russo, D., Fazio, E., Cirrincione, R., & Mamtani, M. A. (2021). Fabric analysis in upper crustal post-collisional granitoids from the Serre Batholith (Southern Italy): Results from microstructural and AMS investigations. *Geosciences (Switzerland)*, *11*(10), 414. https://doi.org/10.3390/geosciences11100414

Fiannacca, P., Williams, I. S., & Cirrincione, R. (2017). Timescales and mechanisms of batholith construction: Constraints from zircon oxygen isotopes and geochronology of the late Variscan Serre Batholith (Calabria, southern Italy). *Lithos*, *277*, 302–314. https://doi.org/10.1016/j.lithos.2016.06.011

Fiannacca, P., Williams, I. S., Cirrincione, R., & Pezzino, A. (2008). Crustal contributions to late Hercynian peraluminous magmatism in the southern Calabria–Peloritani Orogen, southern Italy: Petrogenetic inferences and the Gondwana connection. *Journal of Petrology*, *49*(8), 1497–1514. https://doi.org/10.1093/petrology/egn035

Fiannacca, P., Williams, I. S., Cirrincione, R., & Pezzino, A. (2019). Poly-orogenic melting of metasedimentary crust from a granite geochemistry and inherited zircon perspective (southern Calabria-Peloritani orogen, Italy). *Frontiers in Earth Science*, *7*, 119. https://doi.org/10.3389/feart.2019.00119

Fornelli, A., Festa, V., Micheletti, F., Spiess, R., & Tursi, F. (2020). Building an orogen: Review of U-Pb zircon ages from the calabria-peloritani terrane to constrain the timing of the southern variscan belt. *Minerals*, *10*(11), 944. 1-29. https://doi.org/10.3390/min10110944

Franke, W. (2000). The mid-European segment of the variscides: Tectonostratigraphic units, terrane boundaries and plate tectonic evolution. *Geological Society, London, Special Publications*, *179*(1), 35–61. https://doi.org/10.1144/GSL.SP.2000.179.01.05

Gosso, G., Lardeaux, J.-M., Zanoni, D., Volante, S., Corsini, M., Bersezio, R., Mascle, J., Spaggiari, L., Spalla, M. I., Zucali, M., Giannerini, G., & Camera, L. (2019). Mapping the progressive geologic history at the junction of the alpine mountain belt and the western Mediterranean ocean. *Ofioliti*, *44*(2), 97–110. https://doi.org/10.4454/ofioliti.v44i2.527

Gosso, G., Messiga, B., Rebay, G., & Spalla, M. I. (2010). Interplay between deformation and metamorphism during eclogitization of amphibolites in the Sesia–Lanzo Zone of the Western Alps. *International Geology Review*, *52*(10–12), 1193–1219. https://doi.org/10.1080/00206810903529646

Gosso, G., Rebay, G., Roda, M., Spalla, M. I., Tarallo, M., Zanoni, D., & Zucali, M. (2015). Taking advantage of

petrostructural heterogeneities in subduction collisional orogens, and effect on the scale of analysis. *Periodico di Mineralogia*, *84*(3), 779–825. https://doi.org/10.2451/2015PM0452

Haccard, D., Lorentz, C., & Grandjacquet, C. (1972). Essai sur l'èvolution tectogénétic de la liaison Alpes-Apennines (de la Ligurie à la Calabre). *Memorie della Società Geologica Italiana*, *11*, 309–341.

Heymes, T., Monié, P., Arnaud, N., Pêcher, A., Bouillin, J.-P., & Compagnoni, R. (2010). Alpine tectonics in the Calabrian-Peloritan belt (southern Italy): New 40Ar/39Ar data in the Aspromonte Massif area. *Lithos*, *114*(3-4), 451–472. https://doi.org/10.1016/j.lithos.2009.10.011

Hofmann, M., Linnemann, U., Gerdes, A., Ullrich, B., & Schauer, M. (2009). Timing of dextral strike-slip processes and basement exhumation in the Elbe Zone (Saxo-Thuringian Zone): the final pulse of the Variscan Orogeny in the Bohemian Massif constrained by LA-SF-ICP-MS U-Pb zircon data. *Geological Society, London, Special Publications*, *327*(1), 197–214. https://doi.org/10.1144/SP327.10

Johnson, S. E., & Vernon, R. H. (1995). Inferring the timing of porphyroblast growth in the absence of continuity between inclusion trails and matrix foliations: can it be reliably done? *Journal of Structural Geology*, *17*(8), 1203–1206. https://doi.org/10.1016/0191-8141(95)00021-5

Lardeaux, J. M., & Spalla, M. I. (1991). - From granulites to eclogites in the Sesia zone (Italian Western Alps): a record of the opening and closure of the Piedmont ocean. *Journal of Metamorphic Geology*, *9*(1), 35–59. https://doi.org/10.1111/j.1525-1314.1991.tb00503.x

Liotta, D., Caggianelli, A., Kruhl, J. H., Festa, V., Prosser, G., & Langone, A. (2008). Multiple injections of magmas along a Hercynian mid-crustal shear zone (Sila Massif, Calabria, Italy). *Journal of Structural Geology*, *30*(10), 1202–1217. https://doi.org/10.1016/j.jsg.2008.04.005

Liotta, D., Festa, V., Caggianelli, A., Prosser, G., & Pascazio, A. (2004). Mid-crustal shear zone evolution in a syn-tectonic late Hercynian granitoid (Sila Massif, Calabria, southern Italy). *International Journal of Earth Sciences*, *93*(3), 400–413. https://doi.org/10.1007/s00531-004-0385-8

Malinverno, A., & Ryan, W. B. (1986). Extension in the Tyrrhenian Sea and shortening in the Apennines as result of arc migration driven by sinking of the lithosphere. *Tectonics*, *5*(2), 227–245. https://doi.org/10.1029/TC005i002p00227

Malusà, M. G., Faccenna, C., Baldwin, S. L., Fitzgerald, P. G., Rossetti, F., Balestrieri, M. L., Danišík, M., Ellero, A., Ottria, G., & Piromallo, C. (2015). Contrasting styles of (U) HP rock exhumation along the Cenozoic Adria-Europe plate boundary (Western Alps, Calabria, Corsica). *Geochemistry, Geophysics, Geosystems*, *16*(6), 1786–1824. https://doi.org/10.1002/2015GC005767

Martínez Catalán, J. R., Arenas, R., Abati, J., Martínez, S. S., García, F. D., Suárez, J. F., Cuadra, P. G., Castiñeiras, P., Barreiro, J. G., Montes, A. D., Clavijo, E. G., Pascual, F. J. R., Andonaegui, P., Jeffries, T. E., Alcock, J. E., Fernández, R. D., & Carmona, A. L. (2009). A rootless suture and the loss of the roots of a mountain chain: The Variscan belt of NW Iberia. *Comptes Rendus - Geoscience*, *341*(2–3), 114–126. https://doi.org/10.1016/j.crte.2008.11.004

Matte, P. (2001). The Variscan collage and orogeny (480–290 Ma) and the tectonic definition of the Armorica microplaţe: A review. *Terra nova*, *13*(2), 122–128. https://doi.org/10.1046/j.1365-3121.2001.00327.x

Melleton, J., Cocherie, A., Faure, M., & Rossi, P. (2010). Precambrian protoliths and early Paleozoic magmatism in the French Massif Central: U–Pb data and the North Gondwana connection in the west European Variscan belt. *Gondwana Research*, *17*(1), 13–25. https://doi.org/10.1016/j.gr.2009.05.007

Molli, G., Brogi, A., Caggianelli, A., Capezzuoli, E., Liotta, D., Spina, A., & Zibra, I. (2020). Late Palaeozoic tectonics in Central Mediterranean: A reappraisal. *Swiss Journal of Geosciences*, *113*(1), 23. https://doi.org/10.1186/s00015-020-00375-1

Ortolano, G., Cirrincione, R., & Pezzino, A. (2005). P-T evolution of Alpine metamorphism in the southern Aspromonte Massif (Calabria – Italy). *Schweizerische Mineralogische und Petrographische Mitteilungen*, *85*(1), 31–56.

Ortolano, G., Cirrincione, R., Pezzino, A., & Puliatti, G. (2013). Geo-Petro-Structural study of the Palmi shear zone: Kinematic and rheological implications. *Rendiconti Online della Società Geologica Italiana*, *29*, 126–129.

Ortolano, G., Cirrincione, R., Pezzino, A., Tripodi, V., & Zappala, L. (2015). Petro-structural geology of the Eastern Aspromonte Massif crystalline basement (southern Italy-Calabria): an example of interoperable geo-data management from thin section – to field scale. *Journal of Maps*, *11*(1), 181–200. https://doi.org/10.1080/17445647.2014.948939

Ortolano, G., D'Agostino, A., Pagano, M., Visalli, R., Zucali, M., Fazio, E., Alsop, I., & Cirrincione, R. (2021). Arcstereonet: A New ArcGIS(R) toolbox for projection and analysis of meso- and micro-structural data. *International Journal of Geo-Information*, *10*(2), 50. https://doi.org/10.3390/ijgi10020050

Ortolano, G., Fazio, E., Visalli, R., Alsop, G. I., Pagano, M., & Cirrincione, R. (2020a). Quantitative microstructural analysis of mylonites formed during Alpine tectonics in the western Mediterranean realm. *Journal of Structural Geology*, *131*, 103956. https://doi.org/10.1016/j.jsg.2019.103956

Ortolano, G., Visalli, R., Fazio, E., Fiannacca, P., Godard, G., Pezzino, A., Punturo, R., Sacco, V., & Cirrincione, R. (2020b). Tectono-metamorphic evolution of the Calabria continental lower crust: The case of the Sila Piccola Massif. *International Journal of Earth Sciences*, *109*(4), 1295–1319. https://doi.org/10.1007/s00531-020-01873-1

Padovano, M., Dörr, W., Elter, F. M., & Gerdes, A. (2014). The east Variscan shear zone: Geochronological constraints from the Capo Ferro area (NE Sardinia, Italy). *Lithos*, *196*, 27–41. https://doi.org/10.1016/j.lithos.2014.01.015

Padovano, M., Elter, F. M., Pandeli, E., & Franceschelli, M. (2012). The East Variscan Shear Zone: New insights into its role in the Late Carboniferous collision in Southern Europe. *International Geology Review*, *54*(8), 957–970. https://doi.org/10.1080/00206814.2011.626120

Pereira, M. F., Silva, J. B., Drost, K., Chichorro, M., & Apraiz, A. (2010). Relative timing of transcurrent displacements in northern Gondwana: U–Pb laser ablation ICP-MS zircon and monazite geochronology of gneisses and sheared granites from the western Iberian Massif (Portugal). *Gondwana Research*, *17*(2-3), 461–481. https://doi.org/10.1016/j.gr.2009.08.006

Pezzino, A., Angi, G., Fazio, E., Fiannacca, P., Lo Giudice, A., Ortolano, G., Punturo, R., Cirrincione, R., & de

Vuono, E. (2008). Alpine metamorphism in the aspromonte massif: Implications for a new framework for the southern sector of the Calabria-Peloritani Orogen, Italy. *International Geology Review*, 50(5), 423–441. https://doi.org/10.2747/0020-6814.50.5.423

Pezzino, A., Pannucci, S., Puglisi, G., Atzori, P., Ioppolo, S., & Lo Giudice, A. (1990). Geometry and metamorphic environment of the contact between the Aspromonte – Peloritani Unit (upper unit) and Madonna dei Polsi Unit (lower unit) in the central Aspromonte area (Calabria). *Bollettino della Societa Geologica Italiana*, 109, 455–469.

Platt, J. P., & Compagnoni, R. (1990). Alpine ductile deformation and metamorphism in a Calabrian basement nappe (Aspromonte, south Italy). *Eclogae Geologicae Helvetiae*, 83(1), 41–58. https://doi.org/10.5169/seals-166576

Polino, R., Messina, P., Critelli, S., Putignano, M. L., Minzoni, N., Muto, F., Di Stefano, A., Maniscalco, R., Cirrincione, R., Ortolano, G., Russo, R., Tripodi, V., & Vincenzi, S. (2015). *Carta Geologica d'Italia alla scala 1:50.000 F. 590 Taurianova*. http://www.isprambiente.gov.it/Media/carg/590_TAURIANOVA/Foglio.html

Roda, M., Zucali, M., Corti, L., Visalli, R., Ortolano, G., & Spalla, M. I. (2021). Blueschist mylonitic zones accommodating syn-subduction exhumation of deeply buried continental crust: The example of the Rocca Canavese Thrust Sheets Unit (Sesia–Lanzo Zone, Italian Western Alps). *Swiss Journal of Geosciences*, 114(1), 1–33. https://doi.org/10.1186/s00015-021-00385-7

Romano, V., Cirrincione, R., Fiannacca, P., Lustrino, M., & Tranchina, A. (2011). Late-Hercynian post-collisional dyke magmatism in central Calabria (Serre Massif, southern Italy). *Period Mineral*, 80(3 Special Issue), 489–515. https://doi.org/10.2451/2011PM0032

Rosenbaum, G., Lister, G. S., Duboz, C. (2002). Reconstruction of the tectonic evolution of the western Mediterranean since the Oligocene. In: Reconstruction of the evolution of the Alpine-Himalayan Orogen. *Journal of the Virtual Explorer*, 8, 107–126. https://doi.org/10.3809/jvirtex.2002.00053

Rossetti, F., Faccenna, C., Goffé, B., Monié, P., Argentieri, A., Funiciello, R., & Mattei, M. (2001). Alpine structural and metamorphic signature of the Sila Piccola Massif nappe stack (Calabria, Italy): Insights for the tectonic evolution of the Calabrian Arc. *Tectonics*, 20(1), 112–133. https://doi.org/10.1029/2000TC900027

Rossetti, F., Goffé, B., Monié, P., Faccenna, C., & Vignaroli, G. (2004). Alpine orogenic P-T-t-deformation history of the Catena Costiera area and surrounding regions (Calabrian Arc, southern Italy): The nappe edifice of north Calabria revised with insights on the Tyrrhenian-Apennine system formation. *Tectonics*, 23(6), TC6011, 1–26. https://doi.org/10.1029/2003TC001560

Rottura, A., Bargossi, G. M., Caironi, V., Del Moro, A., Maccarrone, E., Macera, P., Paglionico, A., Petrini, R., Piccareta, G., & Poli, G. (1990). Petrogenesis of contrasting Hercynian granitoids from the Calabrian Arc, southern Italy. *Lithos*, 24(2), 97–119. https://doi.org/10.1016/0024-4937(90)90019-W

Rottura, A., Del Moro, A., Pinarelli, L., Petrini, R., Peccerillo, A., Caggianelli, A., Bargossi, G. M., & Piccarreta, G. (1991). Relationships between intermediate and acidic rocks in orogenic granitoid suites: Petrological, geochemical and isotopic (Sr, Nd, Pb) data from Capo Vaticano (southern Calabria, Italy). *Chemical Geology*, 92(1-3), 153–176. https://doi.org/10.1016/0009-2541(91)90054-U

Spalla, M. I. (1993). Microstructural control on the P-T path construction in metapelites from the Austroalpine crust (Texel Gruppe, Eastern Alps). *Schweizerische Mineralogische und Petrographische Mitteilungen*, 73(2), 259–275. https://doi.org/10.5169/seals-55573

Spalla, M. I., Zucali, M., Di Paola, S., & Gosso, G. (2005). A critical assessment of the tectono-thermal memory of rocks and definition of tectono-metamorphic units: Evidence from fabric and degree of metamorphic transformations. *Geological Society Special Publication*, 243(1), 227–247. https://doi.org/10.1144/GSL.SP.2005.243.01.16

Stampfli, G. M., & Borel, G. D. (2002). A plate tectonic model for the Paleozoic and Mesozoic constrained by dynamic plate boundaries and restored synthetic oceanic isochrons. *Earth and Planetary Science Letters*, 196(1–2), 17–33. https://doi.org/10.1016/S0012-821X(01)00588-X

Stampfli, G. M., & Kozur, H. W. (2006). Europe from the Variscan to the Alpine cycles. *Memoris-Geological Society of London*, 32(1), 57. https://doi.org/10.1144/GSL.MEM.2006.032.01.04

Tartèse, R., Boulvais, P., Poujol, M., Chevalier, T., Paquette, J. L., Ireland, T. R., & Deloule, E. (2012). Mylonites of the South Armorican Shear Zone: Insights for crustal-scale fluid flow and water–rock interaction processes. *Journal of Geodynamics*, 56, 86–107. https://doi.org/10.1016/j.jog.2011.05.003

Tripodi, V., Muto, F., Brutto, F., Perri, F., & Critelli, S. (2018). Neogene-Quaternary evolution of the forearc and backarc regions between the Serre and Aspromonte Massifs, Calabria (southern Italy). *Marine and Petroleum Geology*, 95, 328–343. https://doi.org/10.1016/j.marpetgeo.2018.03.028

Tursi, F., Spiess, R., Festa, V., & Fregola, R. A. (2020). Hercynian subduction-related processes within the metamorphic continental crust in Calabria (southern Italy). *Journal of Metamorphic Geology*, 38(7), 771–793. https://doi.org/10.1111/jmg.12537

von Raumer, J. F., Bussy, F., & Stampfli, G. M. (2009). The Variscan evolution in the external massifs of the Alps and place in their Variscan framework. *Comptes Rendus Geoscience*, 341(2-3), 239–252. https://doi.org/10.1016/j.crte.2008.11.007

von Raumer, J. F., Stampfli, G. M., & Bussy, F. (2003). Gondwana-derived microcontinents – the constituents of the Variscan and Alpine collisional orogens. *Tectonophysics*, 365(1–4), 7–22. https://doi.org/10.1016/S0040-1951(03)00015-5

Zucali, M., Corti, L., Delleani, F., Zanoni, D., & Spalla, M. I. (2020). 3D reconstruction of fabric and metamorphic domains in a slice of continental crust involved in the Alpine subduction system: The example of Mt. Mucrone (Sesia–Lanzo Zone, Western Alps). *International Journal of Earth Sciences*, 109(4), 1337–1354. https://doi.org/10.1007/s00531-019-01807-6

Zucali, M., & Spalla, M. I. (2015). Structural mapping in the Mediterranean: Bridging laboratory to lithosphere. *Journal of Maps*, 11(1), 11–12. https://doi.org/10.1080/17445647.2015.991131

Zucali, M., Spalla, M. I., & Gosso, G. (2002). Strain partitioning and fabric evolution as a correlation tool: The example of the Eclogitic Micaschists Complex in the Sesia-Lanzo Zone (Monte Mucrone-Monte Mars, Western Alps, Italy). *Schweizerische Mineralogische und Petrographische Mitteilungen*, 82(3), 429–454.

Appendices

Appendix 1

Appendix 2